PNNL-27235 Part II

Pacific Northwest
NATIONAL LABORATORY
Proudly Operated by Battelle Since 1965

Transactive System

Part II: Analysis of Two Pilot Transactive Systems using Foundational Theory and Metrics

December 2017

J Lian
Y Sun
D Wu
H Ren
K Kalsi
S Widergren

U.S. DEPARTMENT OF ENERGY

Prepared for the U.S. Department of Energy
under Contract DE-AC05-76RL01830

PACIFIC NORTHWEST NATIONAL LABORATORY
operated by
BATTELLE
for the
UNITED STATES DEPARTMENT OF ENERGY
under Contract DE-AC05-76RL01830

Printed in the United States of America

Available to DOE and DOE contractors from the
Office of Scientific and Technical Information,
P.O. Box 62, Oak Ridge, TN 37831-0062;
ph: (865) 576-8401
fax: (865) 576-5728
email: reports@adonis.osti.gov

Available to the public from the National Technical Information Service
5301 Shawnee Rd., Alexandria, VA 22312
ph: (800) 553-NTIS (6847)
email: orders@ntis.gov <http://www.ntis.gov/about/form.aspx>
Online ordering: http://www.ntis.gov

This document was printed on recycled paper.
(8/2010)

PNNL-27235 Part II

Transactive System

Part II: Analysis of Two Pilot Transactive Systems using Foundational Theory and Metrics

J Lian
Y Sun
D Wu
H Ren
K Kalsi
S Widergren

December 2017

Prepared for
the U.S. Department of Energy
under Contract DE-AC05-76RL01830

Pacific Northwest National Laboratory
Richland, Washington 99352

Summary

The increased penetration of renewable energy has significantly changed the conditions and the operational timing of the electricity grid. More flexible, faster ramping resources are needed to compensate for the uncertainty and variability introduced by renewable energy. Distributed energy resources (DERs) such as distributed generators, energy storage, and controllable loads could help manage the power grid in terms of both economic efficiency and operational reliability. In order to realize the benefits of DERs, coordination and control approaches must be designed to enable seamless integration of DERs into the power grid. Transactive coordination and control is a new approach for DER integration, where individual resources are automated and engaged through market interaction. Transactive approaches use economic signals—prices or incentives—to engage DERs. These economic signals must reflect the true value of the DER contributions, so that they seamlessly and equitably compete for the opportunities that today are only available to grid-owned assets. Value signals must be communicated to the DERs in near-real time, the assets must be imbued with new forms of distributed intelligence and control to take advantage of the opportunities presented by these signals, and they must be capable of negotiating and transacting a range of market-driven energy services. The concepts of transactive energy systems are not new, but build upon evolutionary economic changes in financial and electric power markets. These concepts also recognize the different regional structures of wholesale power markets, electricity delivery markets, retail markets, and vertically integrated service provider markets. Although transactive energy systems are not revolutionary, they will be transformational in their ability to provide flexibility and operational efficiency.

A main goal of this research is to establish a theoretical foundation for analysis of transactive energy systems and to facilitate new transactive energy system design with demonstrable guarantees on stability and performance. Specifically, the goals are to (1) establish a theoretical basis for evaluating the performance of different transactive systems, (2) devise tools to address canonical problems that exemplify challenges and scenarios of transactive systems, and (3) provide guidelines for design of future transactive systems. First, mathematical models for key elements of transactive systems that are consistent with existing control theory need to be developed. In cases where no mathematical treatment is possible under existing control or economic theory, the theory itself must be extended to allow new mathematical models for transactive energy systems. In addition, performance metrics are needed to quantify potential limitations of existing transactive energy systems.

This document is the second of a two-part report. Part 1 reviewed several demonstrations of transactive control and compared them in terms of their payoff functions, control decisions, information privacy, and mathematical solution concepts. It was suggested in Part 1 that these four listed components should be adopted for meaningful comparison and design of future transactive systems. Part 2 proposes qualitative and quantitative metrics that will be needed to compare alternative transactive systems. It then uses the analysis and design principles from Part 1 while conducting more in-depth analysis of two transactive demonstrations: the American Electric Power (AEP) gridSMART Demonstration, which used a double – auction market mechanism, and a consensus method like that used in the Pacific Northwest Smart Grid Demonstration. Ultimately, metrics must be devised and used to meaningfully compare alternative transactive systems. One significant contribution of this report is an observation that the decision function used for thermostat control in the AEP gridSMART Demonstration has superior performance if its decision function is recast to more accurately reflect the power that will be used under for thermostatic control under alternative market outcomes.

Acknowledgments

The authors are grateful to Christopher Irwin of the U.S. Department of Energy Office of Electricity Delivery and Energy Reliability for supporting this research and development effort.

Acronyms and Abbreviations

AEP	American Electric Power
ASW	adjusted social welfare
DER	distributed energy resource
DG	distributed generator
DLC	direct load control
DR	demand response
HVAC	heating, ventilation, and air conditioning
IEEE	Institute of Electrical and Electronics Engineers
LSI	load synchronization index
PRC	price responsive control
PVI	price volatility index
SW	social welfare
VL	violation level

Contents

Summary iii
Acknowledgments v
Acronyms and Abbreviations vii
1.0 Introduction 1
2.0 Performance Metrics 3
2.1 Quantitative Metrics 3
2.2 Qualitative Metrics 5
3.0 Transactive System Analysis for the AEP gridSMART Demonstration 6
3.1 Individual Load Modeling 6
3.2 Local Objective and Control Decision 7
3.3 Coordinator Objective and Control Decision 9
3.4 Practical Bidding Strategy 10
3.5 Proof-of-Concept Verification 12
3.6 Performance Evaluation 13
4.0 Transactive System Analysis for the Pacific Northwest Smart Grid Demonstration Project 18
4.1 Dual Decomposition 18
4.2 Convergence Analysis 21
4.3 Simulation Results 23
5.0 Conclusions and Future Work 28
6.0 References 29

Figures

1. Hierarchical Decision-Making Implemented in the Transactive System Deployed in the AEP gridSMART Demonstration 6
2. Operation of Residential HVAC Units in Cooling Mode 7
3. Local Control Response Curve 8
4. User Interface in the AEP gridSMART Demonstration 9
5. Graphical Illustration of Optimal Market Clearing 10
6. Demand Curve of a Residential HVAC Unit 11
7. Illustration of a Practical Bidding Strategy 11
8. Bidding Strategy in the AEP gridSMART Demonstration 12
9. System Performance on 8/20/2009 with Mild Outside Temperature 12
10. System Performance on 8/16/2009 with High Outside Temperature 13
11. Performance Comparison of Two Bidding Strategies in Terms of ASW 13
12. Robustness of the Transactive System to Load Forecasting Errors 14
13. Robustness of the Transactive System to Communication Packet Drop 15
14. Variation of PVI and LSI with Respect to the Mean Values of Different Distributions of $\boldsymbol{k}$ 16
15. Market Clearing Prices for Different Distributions of $\boldsymbol{k}$ 16
16. Aggregated Controllable Load for Different Distributions of $\boldsymbol{k}$ 17
17. Hierarchical Control Framework for Integrated Coordination between DERs and DR 23
18. IEEE 123-Node Test System 24
19. Base-Case Feeder Load (5-minute average) and Outside Air Temperature 25
20. Desired vs. Resulting Feeder Load (both are 5-minute average) 26
21. Generation Output from DGs 26
22. Load under Each Aggregator 27
23. Indoor Air Temperature of a House under Aggregator 1 27

Tables

1. Generator Parameters 24

1.0 Introduction

Electricity demand has been steadily increasing (EIA 2011). One way to keep up with demand is to build more generation facilities. However, planning generation capacity based on peak demand could leave much generation capacity idle when peak demand increases faster than base demand. A more appealing solution is to integrate renewable energy into the power grid, which could significantly reduce fossil fuel consumption and greenhouse gas emissions. Renewable integration is growing because of environmental concerns and economic requirements. However, integration of extensive renewable energy into the power grid imposes challenges to the conventional supply-side control paradigm. As pointed out in (CAISO 2010, Makarov et al. 2009, Smith et al. 2007), it will substantially increase the need for operational reserves to absorb the variability of renewable energy so that supply and demand balance instantaneously and continuously. If additional reserves are still required to from conventional generators, it will diminish the net carbon benefit from renewable integration, reduce generation efficiency, and eventually become economically untenable.

Besides supply-side control, there has long been interest in using electric loads to help balance supply and demand; this is termed demand-side control. Development of communication and computation techniques enables real-time control of electric loads (Brooks et al. 2010). When properly coordinated and controlled, aggregated end-user loads can provide various grid services that were traditionally provided by generators (Callaway and Hiskens 2011) and satisfy the requirements of speed, accuracy, and magnitude. Because end-user loads usually have large population size and high aggregated ramping rate, demand-side control offers enormous potential to mitigate the variability and uncertainty introduced by renewable generation.

A simple form of aggregated load control is direct load control (DLC), where the aggregator (utility companies, load serving entities, or curtailment service provider) can remotely control end-user loads based on prior mutual financial agreements. Traditional DLC is usually concerned only with services such as peak shaving and load shifting (Chen et al. 1995, Chu et al. 1993, Kurucz et al. 1996). Lately, DLC has begun focusing on modeling and control for a large population of end-user loads such as thermostatically controlled loads (Bashash and Fathy 2013, Callaway 2009, Kalsi et al. 2012, Kondoh et al. 2011, Mathieu et al. 2013, Zhang et al. 2013), plug-in electric vehicles (Liu et al. 2013, Vandael et al. 2013), and data center servers (Chen et al. 2013, Li et al. 2014) to provide services including frequency regulation and load following. Some of these DLC approaches require fast communication between the aggregator and individual loads.

Although DLC can achieve reliable and accurate aggregated load response, its practical application is greatly challenged by privacy and security concerns of residential customers. It is usually difficult in practice to obtain private information that is required for the implementation of DLC approaches. As an alternative to DLC, price responsive control (PRC) protects customer privacy by sending price signals to end-user loads so that they can individually and voluntarily manage their local demand. Common examples of PRC include time-of-use pricing, critical-peak pricing, and real-time pricing (RTP) (Allcott 2011, Borenstein et al. 2002, Chao 2010, Hogan 2010). Recently projects (Faruqui et al. 2010) have demonstrated the performance of PRC in terms of payment reduction, load shifting, and power shaving. However, these approaches either directly pass the wholesale energy price to end users or modify the wholesale price in a heuristic way. Therefore, it cannot achieve the predictable, reliable aggregated load response required of demand-response applications.

Transactive control and coordination is a new type of coordinated load control for demand response. Concepts from microeconomic theory (Mas-Colell et al. 1995) are combined with control theory to design strategies to coordinate and control the aggregated response (Fahrioglu and Alvarado 2000, Samadi et al.

2012). Transactive control has advantages of both PRC and DLC. It preserves customer privacy by using internal price as the control signal. However, the internal price is systematically designed according to specific control objectives, which can be dramatically different from the wholesale price (see, for example, (Chen et al. 2010, Li et al. 2011)). Hence, it can also have more predictable and reliable aggregated load response.

The GridWise® Architecture Council defines transactive energy as, "a system of economic and control mechanisms that allows the dynamic balance of supply and demand across the entire electrical infrastructure using value as a key operational parameter" (The GridWise Architecture Council 2015). Several field demonstration projects in the U.S. and Europe have proven the technology feasibility of transactive energy. The Olympic Peninsula Demonstration (2006–2007) (Fuller et al. 2011, Hammerstrom et al. 2007) was the first proof-of-concept demonstration project in the U.S. that used a double-auction market for congestion management. Building upon the Olympic Peninsula Demonstration, the American Electric Power (AEP) gridSMART® Demonstration (2010–2014) (Widergren et al. 2014, Widergren et al. 2014) also used the double-auction market for residential load coordination and incorporated RTP. The Pacific Northwest Smart Grid Demonstration (2010–2015) (Hammerstrom et al. 2015, Huang et al. 2010) used peer-to-peer negotiation based on consensus principles to coordinate the operation of DERs. PowerMatching City (2009–2015) (Kok et al. 2012) was a demonstration project in Europe that used a double-auction market to balance supply and demand.

In Part I of this report, we first reviewed literature on existing transactive energy systems. Using principles from microeconomic theory, we proposed a unified theoretical foundation for systematic analysis and design of transactive energy systems. In Part II, we develop performance measures for analyzing different transactive approaches and apply the theoretical foundations developed in Part I to analyze transactive energy systems deployed in the AEP gridSMART demonstration and consensus methods like that used in the PNWSGD project.

2.0 Performance Metrics

To evaluate and compare the effectiveness of different transactive designs, some performance metrics must be developed. Because transactive approaches by nature incorporate market principles into their design, some metrics will be generally applicable to any approach. However, due to different control objectives or implementation methods, some metrics might not be applicable to all approaches. In this section, we will define quantitative and qualitative performance metrics to characterize transactive approaches. Usually, qualitative metrics are concerned with perspectives that cannot be fully described by numbers. However, qualitative analysis can often be performed by investigating the sensitivity of specific quantitative metrics under different scenarios. These performance metrics can be used to provide detailed insight into the effectiveness and further identify the limitations of transactive designs. They can also provide guidance to improve the design of future transactive energy systems.

2.1 Quantitative Metrics

It was shown in Part 1 of this report that the control objectives of transactive approaches can be formulated as an optimization problem of maximizing social welfare of the entire system subject to the feeder capacity limit for each market period. Hence, the first metric is ***social welfare*** (*SW*, $) over each market period, which quantifies the optimality of proposed control solutions. For transactive approaches that coordinate generation and load, social welfare is defined as the difference between the total utility of energy consumption and the total cost of energy production:

$$SW = \sum_{i=1}^{N_L} U_i\left(p_i^L\right) - \sum_{j=1}^{N_G} C_j\left(p_j^G\right), \tag{2.1}$$

where $U_i(\cdot)$ are the utility functions of individual load entities, $C_j(\cdot)$ are the cost functions of individual generators, and p_i^L and p_j^G are the average power consumption and production for each market period, respectively. A better transactive design will usually have a higher social welfare during any single time period. For transactive approaches that solve the coordination problem among responsive loads only, social welfare is defined as

$$SW = \sum_{i=1}^{N} U_i\left(p_i\right) - C\left(\sum_{i=1}^{N} p_i\right), \tag{2.2}$$

where $C(\cdot)$ is the cost function of total load consumption, and p_i is the average power consumption of individual loads for each market period.

The next metric is ***violation level*** (*VL*, kW), which measures the severity of power flow constraint violation. For transactive approaches that manage feeder congestion, violation level can be defined as the undesired amount of power exceeding the capacity limit D, that is,

$$VL = \max\left\{0, \sum_{i=1}^{N} p_i - D\right\}, \tag{2.3}$$

where p_i represents the average power of loads on the feeder. Violation level can also be expressed as a percentage of the feeder capacity limit:

$$VL\% = \frac{\max\left\{0,\ \sum_{i=1}^{N} p_i - D\right\}}{D} \times 100\%, \tag{2.4}$$

which is sometimes more convenient and informative.

When the power flow constraints are violated, it is possible to end up with higher *SW* than that without violation because more energy consumption may result in higher utility for the system. Thus, the metrics *SW* and *VL* have to be considered simultaneously for a fair comparison of two approaches. One simple but effective way to reflect their trade-offs in practice is to penalize *SW* by *VL*, which leads to the metric ***adjusted social welfare*** (*ASW*, $) defined as

$$ASW = SW - \omega \cdot VL, \tag{2.5}$$

where ω ($/kW) is the weighting factor for system violations and represents the violation tolerance or penalty in this system. The value of ω should be selected based on the practical application. The larger the weighting factor, the lower the tolerance of system violation.

These quantitative metrics are applicable to transactive and other market-based systems in general. For transactive approaches based on consensus negotiation, the required ***number of iterations*** for each market period is a unique performance metric because the market clearing prices are obtained using iterative algorithms with predefined convergence criteria. If a large number of iterations is required for the market clearing price to converge, the required time for price convergence could exceed the given market period, which is not acceptable.

Besides those metrics that are defined over a single market period, three quantitative metrics that are defined over multiple market periods can also provide useful insights by examining control performance from period to period. The first one is ***total adjusted social welfare*** (*TASW*, $), which represents the total social welfare penalized by violations over an extended time. It is defined as the total sum of ASW over multiple market periods:

$$TASW = \sum_{k=1}^{T} ASW(k), \tag{2.6}$$

where k is the index of the market period and T is the total number of market periods. The second metric is ***price volatility index***, *PVI*, which reflects the degree of volatility in market clearing prices. It is defined as the root-mean-square error between the original and time-shifted market clearing prices over an extended time:

$$PVI = \sqrt{\frac{\sum_{k=1}^{T}\left(\lambda_{\text{clear}}(k) - \lambda_{\text{clear}}(k+1)\right)^2}{T}}, \tag{2.7}$$

where $\lambda_{\text{clear}}(k)$ is the market clearing price. The third metric is ***load synchronization index***, *LSI*, which measures changes in aggregated load. It is defined as the root-mean-square error between the original and time-shifted aggregate load over an extended time:

$$LSI = \sqrt{\frac{\sum_{k=1}^{T}\left(P_{\text{agg}}(k) - P_{\text{agg}}(k+1)\right)^2}{T}}, \tag{2.8}$$

where $P_{\text{agg}}(k)$ is the aggregated load.

2.2 Qualitative Metrics

Qualitative metrics often rely on the calculation of quantitative metrics under different conditions, and actually describe the sensitivity of transactive control systems to practical conditions. One important qualitative metric, for example, is the sensitivity of ***adjusted social welfare*** to the variability and uncertainty that are introduced by imperfect communications, load forecasting errors, and unpredictable customer behaviors.

- Forecasting errors—transactive control systems focus on coordinating and controlling responsive loads. However, the power/energy consumption of both controllable and uncontrollable loads must be forecast during market periods. Thus, the load forecasting errors can significantly affect the effectiveness of the proposed controller.
- Communication system effects—the implementation of transactive control systems is heavily dependent on communication. The underlying controller development usually assumes a perfect communication network that is fast and accurate enough for information exchange. However, communication systems commonly experience network effects such as packet delay, packet drop, and even quantization errors. Unless systematically addressed in controller development, these effects will inevitably affect the performance of transactive control systems.
- Customer behaviors—individual customers are treated as self-interested with private preferences. It is usually assumed that these customers are rational, and willing to provide true information in a market environment. This is only valid if the underlying market is completely competitive. However, complete competitiveness can only be guaranteed in practice by a very large number of market participants. Therefore, there is a chance that individual customers with large market power can manipulate the market prices for their own benefit. This will also significantly affect the controller performance in maximizing global social welfare.

Another important qualitative metric for transactive control systems that is particularly applicable to iterative solution concepts is **scalability** with respect to the number of market participants. This metric will be described by the sensitivity of the **number of iterations** to the number of market participants. Transactive control systems need to be deployable at a wide range of scales, in terms of number of transactive nodes, the geographical areas these nodes cover, the size of their networks, and the number of users they comprise. As new assets are continuously added to the system, the controller has to deal with a rapidly increasing amount of information being exchanged between nodes, and ensure that every iteration be completed within the current market period. If the required **number of iterations** for one transactive control system does not increase faster than the increase of market participants, this system is referred to as scalable.

3.0 Transactive System Analysis for the AEP gridSMART Demonstration

This section examines the transactive energy system deployed by the AEP gridSMART demonstration. This transactive energy system has similar characteristics to those deployed in the Olympic Peninsula Demonstration and PowerMatching City demonstration projects. It is a multi-agent system with two types of agents. Individual residential heating, ventilation, and air conditioning (HVAC) units are device agents that represent the consumers in this system. The operation center is the coordinator agent that represents a double-auction market, and can also be considered as the supplier in this system. The decision-making of this transactive system is implemented hierarchically, as shown in Figure 1. Device agents do not communicate with each other but with the coordinator only, so they do not have any information about other device agents. The coordinator agent receives the bids from device agents to determine the clearing price. Device agents make local control decisions based on the received clearing price only. In the following, we will first apply the proposed theoretical framework to systematically analyze this transactive energy system. Then we will apply the proposed metrics to measure the system performance and identify the associated performance limitations.

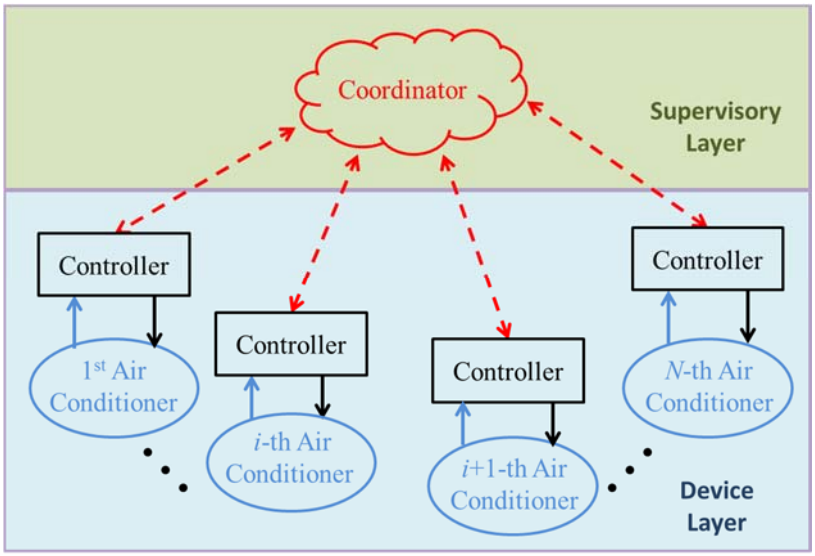

Figure 1. Hierarchical Decision-Making Implemented in the Transactive System Deployed in the AEP gridSMART Demonstration

3.1 Individual Load Modeling

In the AEP gridSMART demonstration, a 5-minute double-auction market is set up for each distribution feeder to coordinate the power demand of feeder loads and keep demand below the capacity limit. The feeder capacity limit is usually imposed by the thermal constraint of the feeder transformer. Among feeder loads, only residential HVAC units are considered controllable loads to provide demand flexibility. A residential HVAC unit is a thermostatically controlled load. It has two operating modes, ON and OFF. As illustrated by Figure 2, switching between two modes is fully dictated by a temperature setpoint T_{set} and a deadband $[-\delta/2, \delta/2]$ centered on the setpoint. When the indoor air temperature rises beyond the upper side of the deadband, the unit turns ON to provide cool air so that the indoor air temperature will decrease. When it drops below the lower side of the deadband, the unit turns OFF so that the indoor air

temperature will rise again. The indoor air temperature oscillates around the setpoint, and the deviation will remain within the deadband.

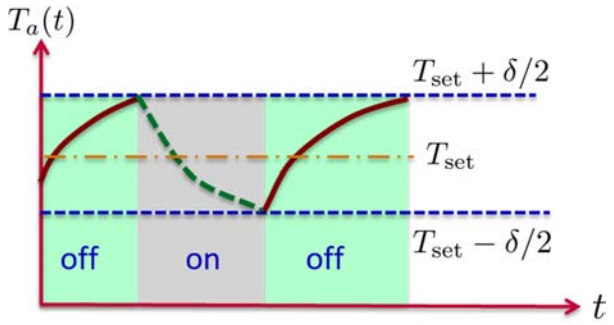

Figure 2. Operation of Residential HVAC Units in Cooling Mode

The dynamics of a residential HVAC unit can be modeled as a switched system with both discrete and continuous states. Many dynamical models are available in the literature with different levels of detail. In this work, we consider the following equivalent thermal parameter model (Zhang et al. 2013),

$$\dot{\boldsymbol{x}}(t) = \begin{cases} \boldsymbol{A}\boldsymbol{x}(t) + \boldsymbol{B}_{\text{on}}, \text{if } q(\text{t}) = 1 \\ \boldsymbol{A}\boldsymbol{x}(t) + \boldsymbol{B}_{\text{off}}, \text{if } q(\text{t}) = 0, \end{cases} \tag{3.1}$$

where $\boldsymbol{x}(t)$ is the continuous state vector consisting of indoor air temperature $T_{\text{a}}(t)$ and mass temperature $T_{\text{m}}(t)$, and $q(t)$ denotes the operating mode of the HVAC unit with $q(t) = 1$ when it is ON and $q(t) = 0$ when it is OFF. The discrete state $q(t)$ is controlled by a hysteretic controller,

$$q(t^+) = \begin{cases} 1, \text{if } T_a(t) \geq T_{\text{set}} + \dfrac{\delta}{2} \\ 0, \text{if } T_a(t) \leq T_{\text{set}} - \dfrac{\delta}{2} \\ q(t), \text{otherwise.} \end{cases} \tag{3.2}$$

Now we will look at the objectives and control decisions of individual agents in more detail.

3.2 Local Objective and Control Decision

The local objective of each device agent is to determine the energy consumption in such a way that local payoff can be maximized for a given market clearing price. This can be mathematically represented as the following payoff maximization problem:

$$\begin{aligned} &\underset{p_i}{\text{Maximize}} && U_i(p_i; \theta_i) - \lambda_c p_i \\ &\text{Subject to} && p_{i,\min} \leq p_i \leq p_{i,\max}. \end{aligned} \tag{3.3}$$

In (3.3), $U_i(p_i; \theta_i)$ is the utility function of energy consumption, p_i denotes the average power[1] within the market period, θ_i represents the private local information, λ_c is the market clearing price, and $p_{i,\min}$ and

[1] The average power and energy consumption for a given period of time are interchangeable.

$p_{i,\max}$ specify the feasible range of average power for each market period. Note that $p_{i,\min}$ is not necessarily zero, and $p_{i,\max}$ is not necessarily the maximum average power unless the unit is to be ON for the entire market period. This is because the current indoor air temperature could be close to the boundaries of the deadband, which prevents the unit from consuming zero or maximum energy in the time period. In general, the utility function $U_i(p_i;\theta_i)$ is concave, continuously differentiable, and furthermore, $U_i(0;\theta_i)=0$ and $U_i'(p_i;\theta_i)>0$. Let $h_i(\lambda_c;\theta_i)$ denote the optimal solution to the maximization problem (3.3), that is,

$$h_i(\lambda_c;\theta_i)=\underset{p_{i,\min}\le p_i\le p_{i,\max}}{\operatorname{argmax}} U_i(p_i;\theta_i)-\lambda_c p_i. \tag{3.4}$$

This optimal solution describes the relationship between the market clearing price and the optimal energy allocation, which is often referred to as the demand curve. As will be seen later, individual demand curves are required for the market to clear. However, the demand curve cannot be obtained by solving the above payoff maximization problem because the utility function is locally unknown. In fact, it is not straightforward to construct the utility functions of controllable loads. The cost functions for fueled generators can be easily determined based on the operational cost, fuel efficiency, and fuel cost of individual generators. However, individual utility functions depend on the household owners' preferences, which are usually very hard to characterize.

In this demonstration project, the temperature setpoint T_{set} is the local control input. It is updated inside the thermostat every five minutes in response to the received market clearing price. The mapping from the clearing price to the new temperature setpoint is specified by the local control response curve, as shown in Figure 3, which is determined by several parameters.

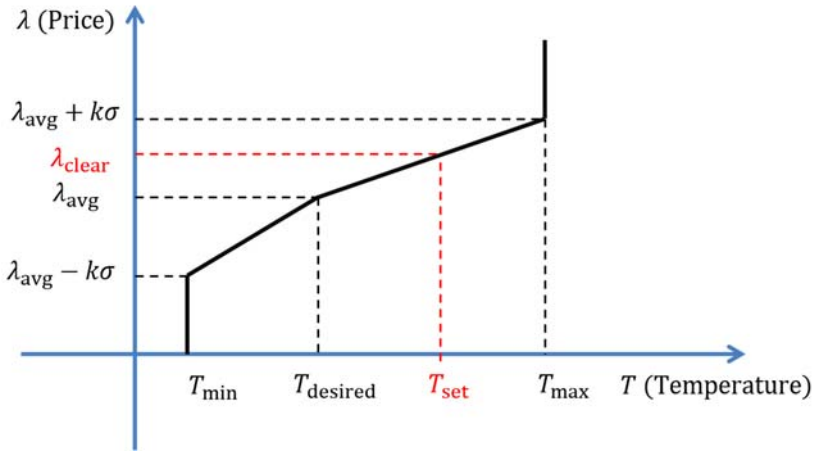

Figure 3. Local Control Response Curve

The parameters λ_{avg} and σ are the average and standard deviation, respectively, of the market clearing prices over a past period. They can be easily obtained by adding memory to the thermostat so that it can keep track of historical clearing prices. The parameters T_{desired}, $T_{\min}$, and $T_{\max}$ are specified by the household occupant directly, where T_{desired} is the ideal indoor air temperature setpoint, and $T_{\min}$ and $T_{\max}$ are the lower and upper bounds of the acceptable indoor air temperature setpoint. The parameter k is specified by the household occupant through a sliding bar as shown in Figure 4, which represents the occupant's preference for comfort vs. cost. A positive number will be abstracted from the household occupant's preference. For example, when k is very large, the response curve becomes an almost vertical line at T_{desired}. This implies that the household occupant is very sensitive to the indoor air temperature,

and would like to maintain the setpoint at T_{desired} regardless of the clearing price. When k very small, the response curve becomes an almost horizontal line at λ_{avg}. This implies that the household occupant is very sensitive to the electricity price, and would like to sacrifice comfort for cost savings.

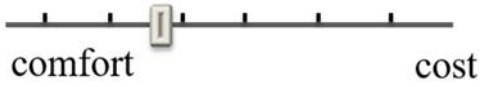

Figure 4. User Interface in the AEP gridSMART Demonstration

3.3 Coordinator Objective and Control Decision

The objective of the coordinator agent is to achieve energy allocation in such a way that total system cost is minimized while the feeder capacity limit is respected. Furthermore, the resulting energy allocation must be realized by a uniform clearing price for all responsive loads. This objective can be mathematically represented as an optimization problem:

$$\begin{aligned} \underset{p_i}{\text{Maximize}} \quad & \sum_{i=1}^{N} U_i(p_i;\theta_i) - C\left(\sum_{i=1}^{N} p_i\right) \\ \text{Subject to} \quad & \sum_{i=1}^{N} p_i \le D \\ & p_{i,\min} \le p_i \le p_{i,\max} \\ & p_i = h_i(\lambda_c;\theta_i) \end{aligned} \tag{3.5}$$

where D represents the feeder capacity limit for controllable loads and $C\left(\sum_{i=1}^{N} p_i\right)$ denotes the cost function of total energy consumption for this distribution feeder. The control decision of the coordinator agent is a uniform market clearing price λ_c. Mathematically, it can be shown that the optimal solution to (3.5) is also the optimal solution to the following optimization problem:

$$\begin{aligned} \underset{p_i}{\text{Maximize}} \quad & \sum_{i=1}^{N} U_i(p_i;\theta_i) - C\left(p_0\right) \\ \text{Subject to} \quad & \sum_{i=1}^{N} p_i = p_0 \\ & p_0 \le D \\ & p_{i,\min} \le p_i \le p_{i,\max}, \end{aligned} \tag{3.6}$$

where the dual variable associated with the equality constraint $\sum_{i=1}^{N} p_i = p$ is the uniform market clearing price λ_c. The optimization problem (3.6) is actually a social welfare maximization problem involving a number of customers and one supplier. Therefore, if the coordinator agent knows the cost function and individual utility functions, it can easily determine the market clearing price λ_c by solving (3.6).

However, practical implementation requires determination of the market clearing price through the bidding and clearing process instead of collecting individual utility functions from device agents.

It is shown in (Li et al. 2016) that, as long as the demand function $h_i(\lambda_c, \theta_i)$ is continuous and nonincreasing, this transactive system can achieve a competitive equilibrium if individual device agents submit their demand functions $h_i(\lambda_c; \theta_i)$ as the bidding information, and, at the same time, the market clearing price is calculated as the following:

$$\lambda_c^* = \max\{\bar{\lambda}, \lambda^*\}$$
$$\sum_{i=1}^{N} h_i(\bar{\lambda}, \theta_i) = D \tag{3.7}$$
$$\lambda^* = C'\left(\sum_{i=1}^{N} p_i^*\right)$$

which is graphically illustrated in Figure 5. There are two situations under consideration. When there is no congestion, the clearing price will be equal to the base price. When there is congestion, the clearing price will be higher than the base price so that the total demand can be capped by the capacity limit.

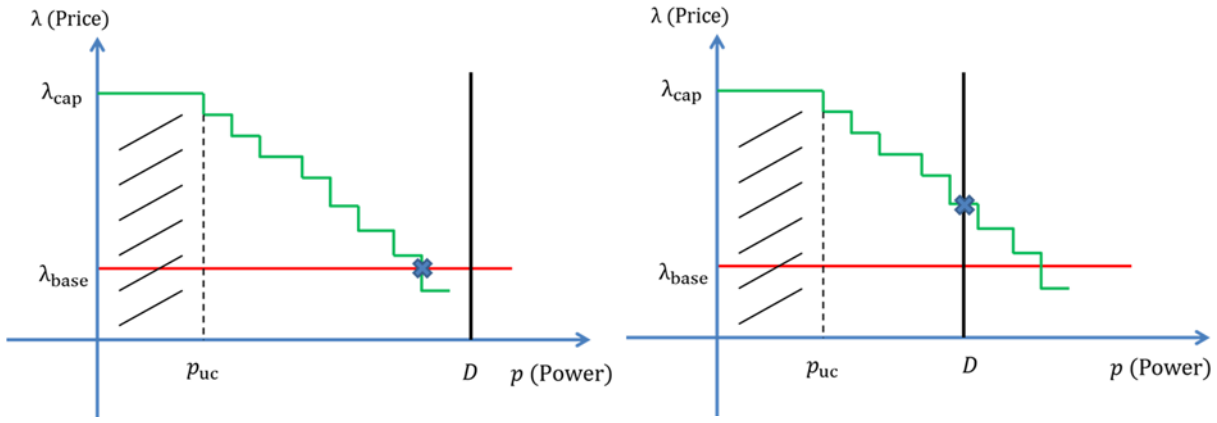

(a) Uncongested case (b) Congested case

Figure 5. Graphical Illustration of Optimal Market Clearing

3.4 Practical Bidding Strategy

The key point for this transactive system to achieve competitive equilibrium is that individual device agents can determine their demand functions $h_i(\lambda_c; \theta_i)$. However, demand functions cannot be obtained by solving the optimization problem (3.6) because the utility function $U_i(p_i; \theta_i)$ is unknown. Recall that the local control response curve is built to describe the relationship between the market clearing price and the local temperature setpoint. The construction of this response curve actually provides a way to quantify the preference of household owners. Hence, there is an alternative way to easily determine the demand curve without solving the above optimization problem. For a given temperature setpoint, the energy consumption for the next market cycle can be calculated if we know the thermal dynamics as described by the equivalent thermal parameter model and the current indoor air temperature. On the other hand, for a given market clearing price, the temperature setpoint can be calculated based on the local control

response curve. By considering these two relationships together, we can obtain the relationship between the clearing price and the energy consumption over the next market cycle, which is exactly the demand curve as defined by the solution $h_i(\lambda_c; \theta_i)$. An example demand curve of a residential HVAC unit is given in Figure 6. This demand curve is continuous and nonincreasing with respect to the clearing price. When the clearing price is high, the residential HVAC unit tends to reduce the energy consumption to save money. When the clearing price is low, it tends to consume more energy so that it can save money by preconditioning the indoor air.

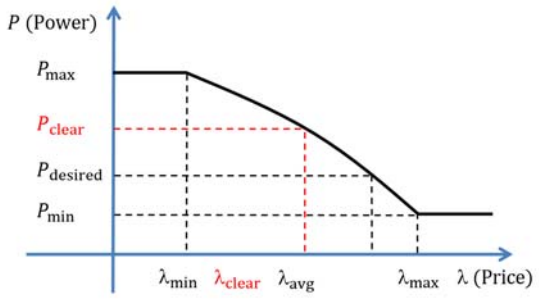

Figure 6. Demand Curve of a Residential HVAC Unit

Although it is desired that individual device agents submit their demand function $h_i(\lambda_c; \theta_i)$ directly, considerable communication is needed for device agents to submit the entire demand functions. Therefore, in order to reduce the burden on the communication link, the demand function can be approximated by a step function, as illustrated by Figure 7, so that the bidding information will be only a set of numbers including bidding price and quantity. In this case, there will be two pairs of price and quantity: $(\lambda_{\text{bid}}, P_{\max})$ and $(\lambda_{\text{bid}}, P_{\min})$.

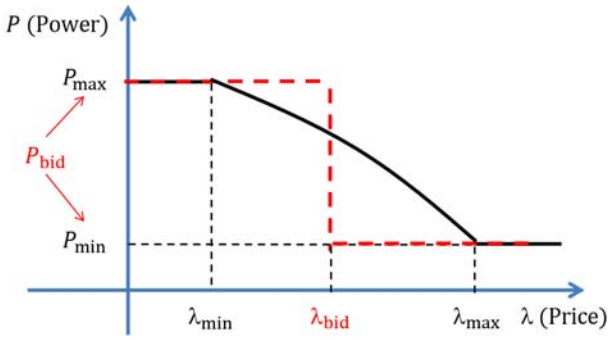

Figure 7. Illustration of a Practical Bidding Strategy

When compared to the bidding strategy deployed in the AEP gridSMART demonstration, which is shown in Figure 8, we can easily see that the original bidding strategy does not reveal the true information of the local demand for the coming market cycle. In the AEP gridSMART demonstration bidding strategy, the bidding price is calculated from the same local control response curve based on the current indoor air temperature. This bidding strategy will be accurate if there is no deadband associated with the operation of residential HVAC units. When a deadband is involved, one unit will not immediately turn OFF if it bids lower than the clearing price. Similarly, it will not immediately turn ON if it bids higher than the clearing price. The actual switching of operating modes depends on the relative distance between the current indoor air temperature and the new temperature setpoint. Thus, we can expect that the feeder capacity limit may still be violated from time to time during system operation with the original bidding strategy.

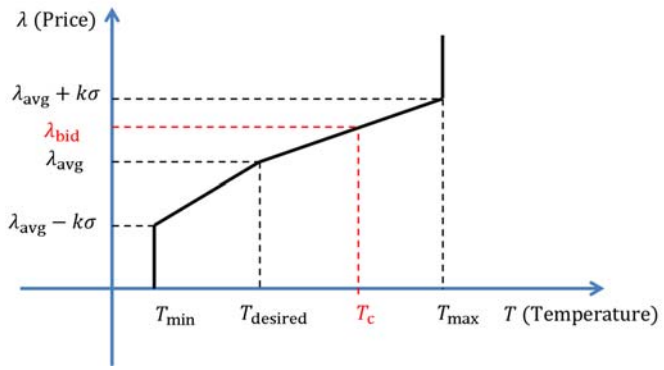

Figure 8. Bidding Strategy in the AEP gridSMART Demonstration

3.5 Proof-of-Concept Verification

In this section, we use a simulation study to verify our discovery regarding the bidding problem in the AEP gridSMART demonstration. In this study, we considered a distribution feeder with 1000 residential HVAC units of different rated power randomly distributed around 5 kW. The total amount of uncontrollable loads on the same feeder was set at 12 MW, and the distribution feeder capacity limit was assumed to be 15 MW. The retail price (base price) used in the simulation was derived from PJM's wholesale energy market and modified as defined by AEP's tariff. We considered the system operation on 8/20/2009 with mild outside temperature, and on 8/16/2009 with high outside temperature. The weather data were the actual records for Columbus, Ohio.

The simulation results shown in Figure 9 and Figure 10 confirm our discovery regarding the issue associated with the original bidding strategy in the AEP gridSMART demonstration. We can see that the original bidding strategy fails to maintain the total demand below the feeder capacity limit. The capacity constraint violation becomes more severe when the outside temperature is high because there is more demand for HVAC during a hot day. With the improved bidding strategy, the system can successfully resolve the feeder congestion and maintain the total feeder power below the feeder capacity limit.

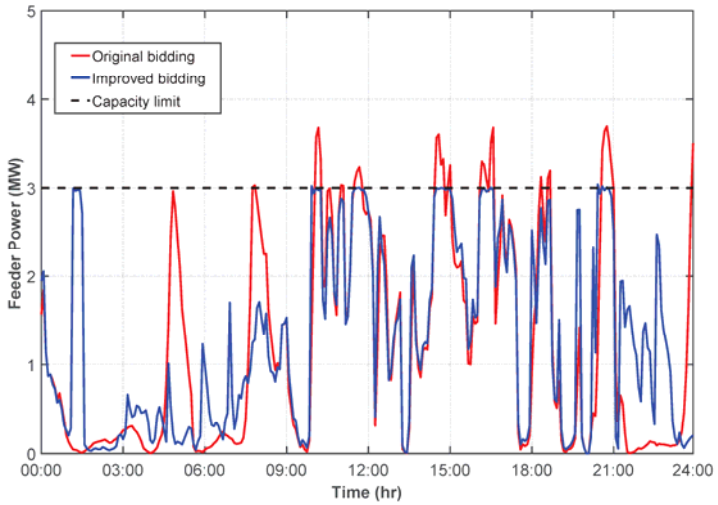

Figure 9. System Performance on 8/20/2009 with Mild Outside Temperature

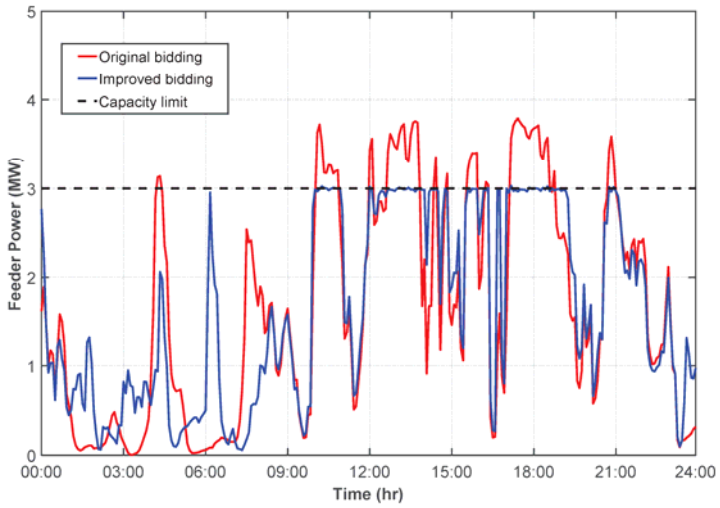

Figure 10. System Performance on 8/16/2009 with High Outside Temperature

3.6 Performance Evaluation

In the following, the performance metrics proposed in Section 2.0 will be used to systematically evaluate the performance of the transactive system in the AEP gridSMART demonstration. Sensitivity studies will also be performed with these metrics to identify the design limitations of this transactive energy system to improve future designs for practical deployment.

We first compare the economic performance of this transactive system with both the original and the improved bidding strategies. The simulation results are shown in Figure 11, where the violation factor penalty ω is selected to be 0.01 $/kW. The transactive system with the improved bidding strategy can achieve higher adjusted social welfare, and thus has better economic performance than that with the original bidding strategy.

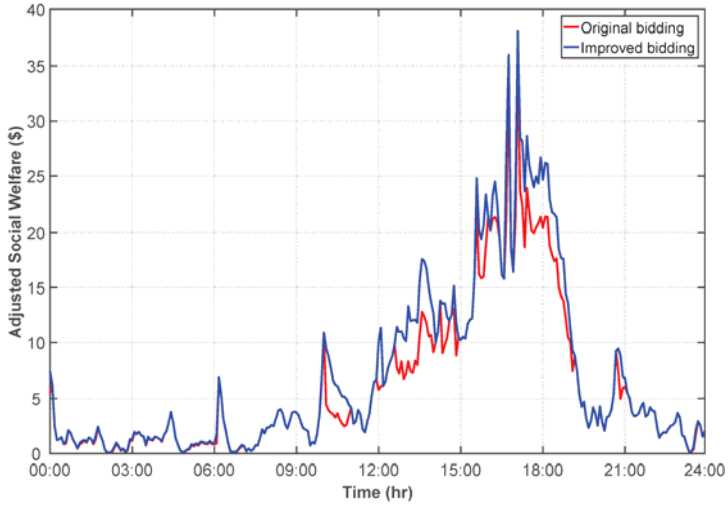

Figure 11. Performance Comparison of Two Bidding Strategies in Terms of ASW

Next we examine the robustness of this transactive system with the improved bidding strategy to two practical conditions during real implementation: the forecasting error of uncontrollable loads and the information loss over the communication link.

Transactive control systems focus on coordinating and controlling responsive loads. However, the energy consumption of uncontrollable loads must be forecasted for the coming market periods. Thus, load forecasting errors can significantly affect the effectiveness of the proposed controller. Simulated load forecasting error is shown in Figure 12, where the market period is at 2:00 p.m. and we consider forecasting error up to ±10%. The performance of this transactive system is sensitive, and thus less robust to the forecasting errors of uncontrollable loads. In particular, it is more sensitive to underestimation of uncontrollable load. Hence, when it is not possible to obtain an accurate estimation of uncontrollable loads in practical applications, it is more conservative to overestimate uncontrollable loads.

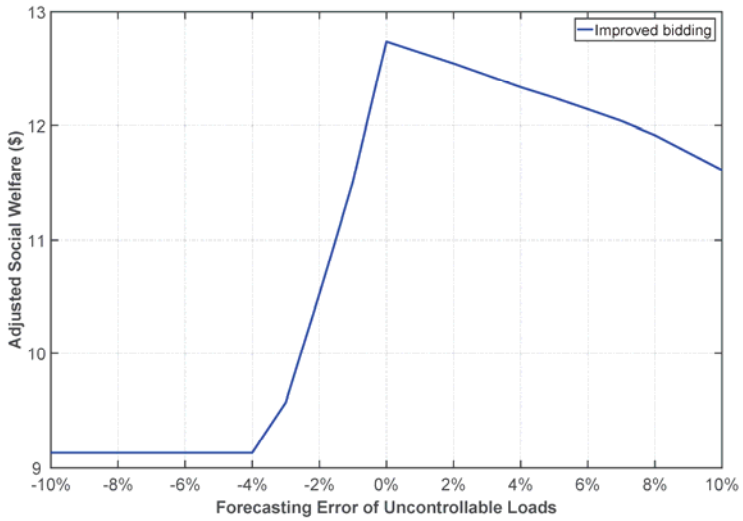

Figure 12. Robustness of the Transactive System to Load Forecasting Errors

The implementation of transactive control systems is heavily dependent on communication. The transactive controller design often assumes a perfect communication network that is fast and accurate enough for information exchange. However, packet delay, packet drop, and even quantization errors occur. Unless systematically taken into account in controller development, these network effects will affect the performance of transactive systems. Simulation results are shown in Figure 13, where we consider packet drop rates up to 20%. Figure 13(a) shows that when the lost bids are replaced by the bids from the previous market period, the transactive system is somewhat robust to this imperfect communication link. However, when the lost bids are not replaced at all, that is, the corresponding residential HVAC units are treated as uncontrollable loads, the transactive system is very sensitive to this imperfect communication link. Therefore, for practical implementation, historical information should be used to replace lost bids.

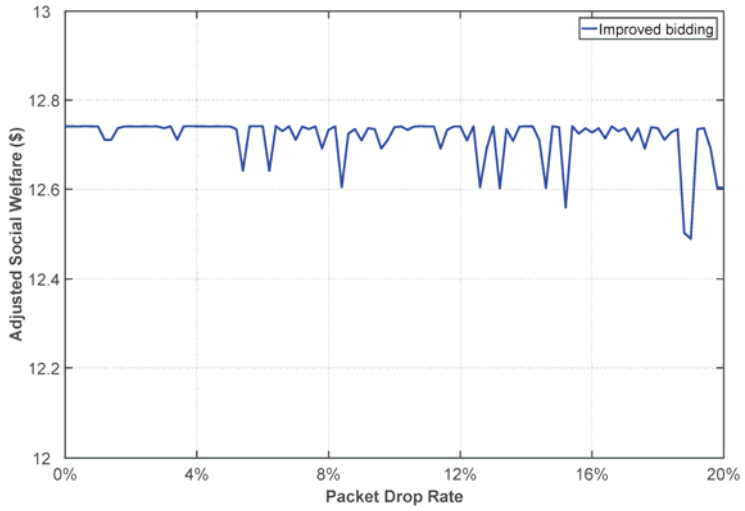

(a) Lost bids are replaced by the bids from the previous market period

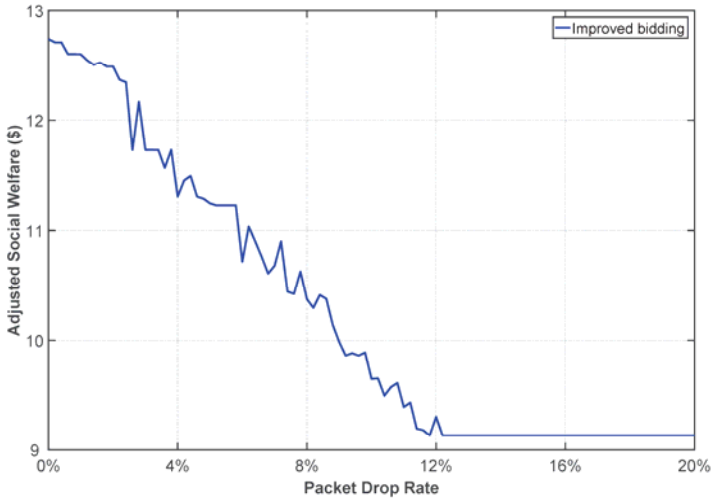

(b) Lost bids are not replaced at all

Figure 13. Robustness of the Transactive System to Communication Packet Drop

Finally, we examine the performance of this transactive system with the improved bidding strategy in terms of price volatility and load synchronization. We investigate how the preferences of individual household occupants contribute to the volatility of the market clearing price and the oscillation of the aggregated load. Recall that the preference of each household occupant is abstracted by a positive number k. When k is small, the household is more sensitive to price fluctuation and thus prefers cost saving to comfort. When k is large, the household is more sensitive to indoor air temperature fluctuation, and thus prefers indoor comfort to cost saving. We evaluate the PVI and LSI of this transactive system for different distributions of k over a range between 1 and 60; the simulation results regarding the variation of PVI and LSI are given in Figure 14. The corresponding market clearing prices and aggregated load are shown in Figure 15 and Figure 16, respectively. While large values of k more successfully moderate prices, small values of k lead to more oscillation of the market clearing price and aggregated load in general. That is, if individual households prefer cost saving to indoor comfort, the market clearing price and aggregated load are more prone to oscillation.

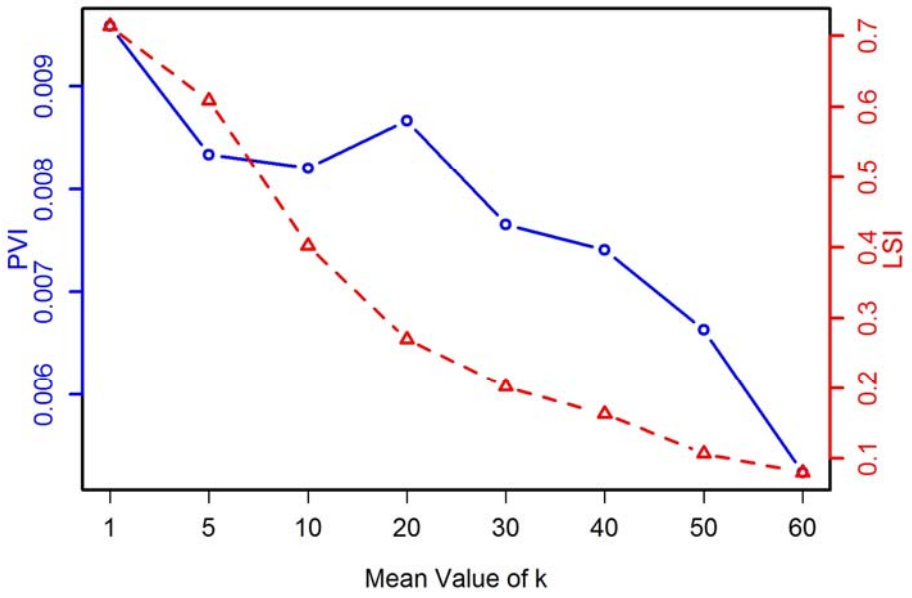

Figure 14. Variation of PVI and LSI with Respect to the Mean Values of Different Distributions of ***k***

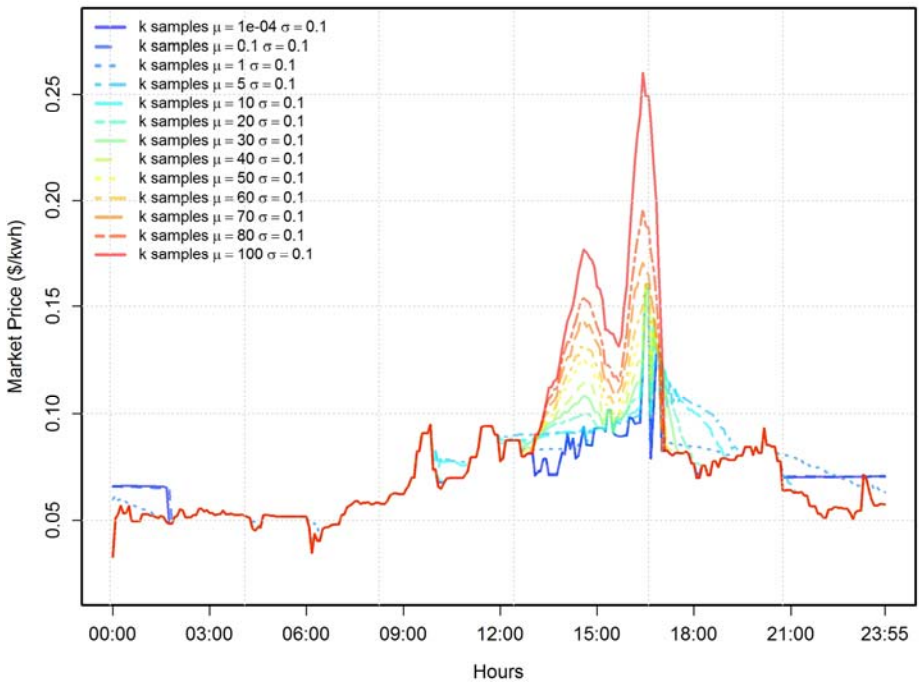

Figure 15. Market Clearing Prices for Different Distributions of ***k***

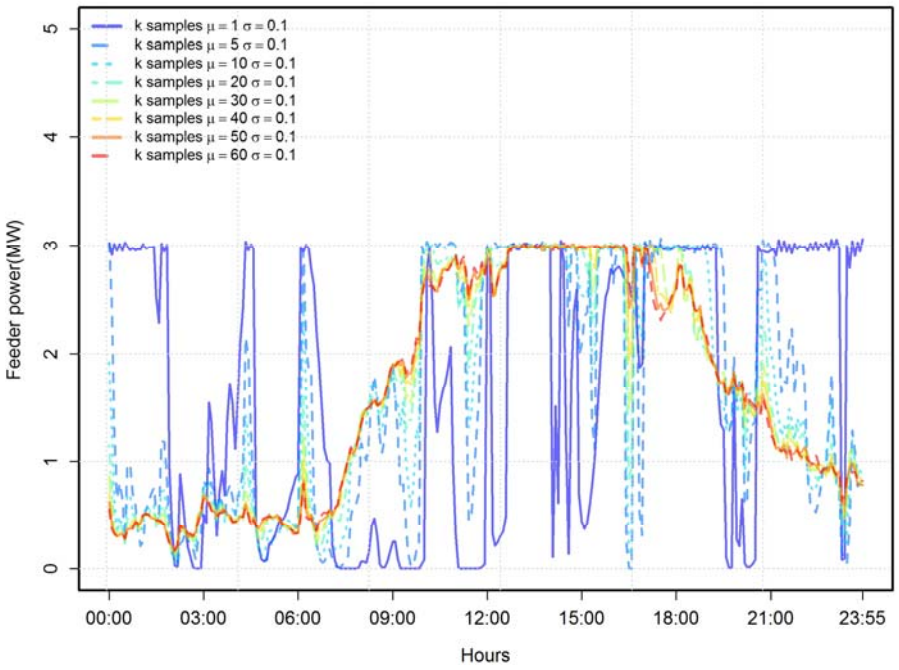

Figure 16. Aggregated Controllable Load for Different Distributions of ***k***

4.0 Transactive System Analysis for the Pacific Northwest Smart Grid Demonstration Project

In the transactive energy system deployed in the Pacific Northwest Smart Grid Demonstration project, market clearing prices are not determined through market bidding and clearing. Instead, individual resources interact with their neighboring resources, which are electrically connected, to exchange information about the quantity and cost of energy produced or consumed. During the information exchange, they make sure that their local objectives and flexibility are properly reflected in the negotiation. Furthermore, information exchange could involve a time series of information so that individual resources can negotiate their operations not only in the next time interval but also over a time horizon. This negotiation continues until the difference of the market clearing price between neighboring resources converges.

In the following, we will apply the proposed theoretical framework to explain the underlying principles of negotiation-based transactive energy systems in general. We will first introduce dual decomposition, which is used for development of all the negotiation algorithms. Then we will discuss the convergence of different methods. Finally, we will provide simulation results to demonstrate the practical application of this type of transactive energy system.

4.1 Dual Decomposition

A transactive energy system that relies on negotiation to determine market clearing prices is also a multi-agent system with two types of agents: the electricity supplier, and the electricity consumer with controllable demand. Individual agents can communicate with their neighboring agents, which are defined based on the connectivity imposed by the communication topology.

For the i-th consumer agent, the local objective is to determine the energy consumption in a way that maximizes local payoff for each market clearing price without violating local constraints. This can be mathematically represented as the following payoff maximization problem:

$$\begin{aligned} &\underset{p_i}{\text{Maximize}} && U_i(p_i;\theta_i) - \lambda_i p_i \\ &\text{Subject to} && p_{i,\min} \le p_i \le p_{i,\max} \end{aligned} \tag{4.1}$$

where $U_i(p_i;\theta_i)$ is the utility function of energy consumption, p_i denotes the average power consumption within the market period, θ_i represents the private local information, λ_i is the market clearing price for energy consumption, and $p_{i,\min}$ and $p_{i,\max}$ specify the minimum and maximum values of average power consumption for each market period, respectively.

For the j-th supplier agent, the local objective is to determine the energy generation in a way that minimizes local cost for each market clearing price without violating local constraints. This can be mathematically represented as the following cost minimization problem:

$$\begin{aligned} &\underset{p_j}{\text{Minimize}} && C_j(p_j;\theta_j) - \lambda_j p_j \\ &\text{Subject to} && p_{j,\min} \le p_j \le p_{j,\max}, \end{aligned} \tag{4.2}$$

where $C_j(p_j;\theta_j)$ is the cost function of energy generation, p_j denotes the average power generation within the market period, θ_j represents the private local information, λ_j is the market clearing price for energy generation, and $p_{j,\min}$ and $p_{j,\max}$ specify the minimum and maximum values of average power generation for each market period, respectively.

At the system level, the global objective is to achieve energy allocation in a way that minimizes total system cost while global constraints are met. For simplicity in the following illustration, the global constraint is selected to be energy balance. Then the global objective can be mathematically represented as the following optimization problem:

$$\begin{aligned} \underset{p_i,p_j}{\text{Minimize}} \quad & \sum_{j=1}^{N_G} C_j(p_j;\theta_j) - \sum_{i=1}^{N_L} U_i(p_i;\theta_i) \\ \text{Subject to} \quad & \sum_{j=1}^{N_G} p_j - \sum_{i=1}^{N_L} p_i = D \\ & p_{j,\min} \le p_j \le p_{j,\max}, \end{aligned} \tag{4.3}$$

where N_G is the number of electricity supliers, N_L is the number of electricity consumers, and D is the uncontrollable demand of the system. For each market period, the goal is to determine the market clearing prices λ_i and λ_j for both electricity consumers and suppliers through peer-to-peer negotiation such that the global objective as defined by (4.3) can be achieved. Therefore, appropriate negotiation algorithms are the key to this type of transactive energy systems.

Note that the market clearing prices λ_i and λ_j are actually dual variables associated with the equality constraints in (4.3). To proceed, consider the following dual problem associated with (4.3):

$$\underset{\lambda}{\text{Maximize}} \quad g(\lambda), \tag{4.4}$$

where $g(\lambda)$ is the dual function defined as the optimal value of the following optimization problem:

$$\begin{aligned} \underset{p_i,p_j}{\text{Minimize}} \quad & \sum_{j=1}^{N_G} C_j(p_j;\theta_j) - \sum_{i=1}^{N_L} U_i(p_i;\theta_i) + \lambda\left(D - \sum_{j=1}^{N_G} p_j + \sum_{i=1}^{N_L} p_i\right) \\ \text{Subject to} \quad & p_{i,\min} \le p_i \le p_{i,\max} \\ & p_{j,\min} \le p_j \le p_{j,\max}. \end{aligned} \tag{4.5}$$

We assume that the cost function $C_j(p_j;\theta_j)$ is convex and the utility function $U_i(p_i;\theta_i)$ is concave. Then it follows from the convexity of problem (4.3) that strong duality holds, that is, there is no duality gap between problem (4.3) and problem (4.4). Because the optimization problem (4.5) is separable with respect to p_i and p_j, the dual function $g(\lambda)$ can be rewritten as

$$g(\lambda) = \sum_{j=1}^{N_G} p_j^*(\lambda) - \sum_{i=1}^{N_L} p_i^*(\lambda) + \lambda D, \tag{4.6}$$

where

$$p_j^*(\lambda) = \underset{p_{j,\min} \le p_j \le p_{j,\max}}{\operatorname{argmin}} \; C_j(p_j; \theta_j) - \lambda p_j \tag{4.7}$$

and

$$p_i^*(\lambda) = \underset{p_{i,\min} \le p_i \le p_{i,\max}}{\operatorname{argmax}} \; U_i(p_i; \theta_i) - \lambda p_i. \tag{4.8}$$

If we also assume that $C_j(p_j; \theta_j)$ and $U_i(p_i; \theta_i)$ are both differentiable, it can be shown that

$$p_j^*(\lambda) = \left(C_j'\right)^{-1}(\lambda), \, p_{j,\min} \le p_j^* \le p_{j,\max} \tag{4.9}$$

and

$$p_i^*(\lambda) = (U_i')^{-1}(\lambda), \, p_{i,\min} \le p_i^* \le p_{i,\max}, \tag{4.10}$$

where $C_j'(p_j; \theta_j)$ and $U_i'(p_i; \theta_i)$ denote the derivatives of $C_j(p_j; \theta_j)$ and $U_i(p_i; \theta_i)$, respectively. Therefore, the dual problem (4.4) can be rewritten as

$$\underset{\lambda}{\text{Maximize}} \quad \sum_{j=1}^{N_G} \left(C_j'\right)^{-1}(\lambda) - \sum_{i=1}^{N_L} (U_i')^{-1}(\lambda) + \lambda D. \tag{4.11}$$

The dual problem (4.11) can be solved iteratively by the following dual decomposition algorithm:

- For the k-th iteration, determine $p_j^*(k)$ and $p_i^*(k)$ from (4.7) and (4.8) with given $\lambda(k)$, respectively;
- Update the market clearing price $\lambda(k)$ using a subgradient method,

$$\lambda(k+1) = \lambda(k) - \alpha \, \partial g(\lambda(k)), \tag{4.12}$$

where $\alpha > 0$ is a prespecified step size, and $\partial g(\lambda)$ is a subgradient of $-g(\lambda)$ defined as

$$\partial g(\lambda(k)) = \sum_{j=1}^{N_G} p_j^*(k) - \sum_{i=1}^{N_L} p_i^*(k) - D; \tag{4.13}$$

- Repeat the above for the $(k+1)$-th iteration until $\lambda(k)$ converges.

In fact, if individual agents can estimate $\partial g(\lambda(k))$ locally, they can update $\lambda(k)$ without the need of a central coordinator. It has been shown that either average consensus algorithms (Zhang and Chow 2011, Zhang and Chow 2012a, Zhang and Chow 2012b) or ratio consensus algorithms (Dominguez-Garcia et al. 2012, Yang et al. 2016) can be used to develop peer-to-peer negotiation algorithms based on the above dual decomposition.

4.2 Convergence Analysis

For practical applications, peer-to-peer negotiation must converge within a finite number of iterations. That is, the optimal solution should be reached within the time duration of each market period. Otherwise, the negotiation between individual agents fails and the resulting market clearing price will not guarantee system optimality. Hence, it is essential to perform convergence analysis on the proposed negotiation algorithms to determine whether they will converge and what the convergence rate will be. In the following, we present convergence analysis of negotiation algorithms for a simplified version of the problem defined by (4.1)-(4.3) to illustrate the particularity and difficulty of this process. As the complexity of the problem setup increases, the associated convergence analysis becomes very complicated or even intractable for practical applications.

Consider a case with N_G electricity suppliers without local constraints and with all electricity demand uncontrollable. Then the local objective of the j-th supplier is

$$\underset{p_j}{\text{Minimize}} \quad C_j(p_j;\theta_j) - \lambda_j p_j, \tag{4.14}$$

and the system-level global objective is

$$\underset{p_j}{\text{Minimize}} \quad \sum_{j=1}^{N_G} C_j(p_j;\theta_j) \tag{4.15}$$

$$\text{Subject to} \quad \sum_{j=1}^{N_G} p_j = D.$$

The dual problem corresponding to problem (4.15) is defined as

$$\underset{\lambda}{\text{Maximize}} \quad g(\lambda) = \sum_{j=1}^{N_G} p_j^*(\lambda) + \lambda D, \tag{4.16}$$

where $p_j^*(\lambda) = \underset{p_j}{\text{argmin}}\, C_j(p_j;\theta_j) - \lambda p_j$, and it can be solved by the following iterative algorithm:

$$\lambda(k+1) = \lambda(k) - \alpha\, \partial g(\lambda(k)), \tag{4.17}$$

where

$$\partial g(\lambda(k)) = \sum_{j=1}^{N_G} p_j^*(k) - D. \tag{4.18}$$

In the following, we assume that the price $\lambda(k)$ is centrally updated. If distributed algorithms are used to estimate the subgradient locally, additional complexity will be added to the convergence analysis. We also assume that the function $-g(\lambda)$ is convex and differentiable. Then the subgradient $\partial g(\lambda)$ is equal to the gradient of $-g(\lambda)$, which is denoted $\nabla g(\lambda)$. Furthermore, we assume that $\nabla g(\lambda)$ is Lipschitz continuous with a constant $L > 0$, that is,

$$|\nabla g(x) - \nabla g(y)| \leq L|x - y|, \forall x, y. \tag{4.19}$$

The detailed convergence analysis for the iterative algorithm (4.17) with imposed assumptions can be found in (Boyd and Vandenberghe 2004). Some important results are summarized and illustrated in the following.

There are different methods of determining the step size α to use in the iterative algorithm (4.17). One of the methods is the fixed step size, where the step size α for each iteration is selected to be a constant value for simplicity. However, it is not easy to determine the appropriate step size in practice. When it is too small, the algorithm will converge very slowly. When it is too large, the algorithm may diverge. It can be shown that under the above assumptions the iterative algorithm (4.17) with $\alpha < 2/L$ will converge to the optimal price λ^*. Moreover, the convergence rate with $\alpha < 1/L$ can be determined as

$$g(\lambda^*) - g\big(\lambda(k)\big) \leq \frac{|\lambda(0) - \lambda^*|^2}{2\alpha k}, \tag{4.20}$$

where $\lambda(0)$ is the initial guess of the price. It follows that when the Lipschitz constant L becomes larger, the step size α must be smaller to guarantee convergence of this algorithm. When the number of electricity suppliers N_G is large, the resulting Lipschitz constant L is usually large as well. Then a very small step size α must be chosen. To better illustrate this result, suppose the cost functions are of the following quadratic form:

$$C_j\big(p_j; \theta_j\big) = a_j p_j^2 + b_j p_j + c_j. \tag{4.21}$$

Then the dual function $g(\lambda)$ can be determined as

$$g(\lambda) = \lambda D - \sum_{j=1}^{N_G} \left(\frac{\big(\lambda - b_j\big)^2}{4a_j} - c_j \right), \tag{4.22}$$

and the gradient $\nabla g(\lambda)$ of $-g(\lambda)$ can be determined as

$$\nabla g(\lambda) = \sum_{j=1}^{N_G} \frac{\lambda - b_j}{2a_j} - D. \tag{4.23}$$

It follows that the Lipschitz constant L is given by

$$L = \sum_{j=1}^{N_G} \frac{1}{2a_j}. \tag{4.24}$$

Hence, as the value of N_G increases, the magnitude of L increases, and the threshold value for step size α, that is, $2/L$, decreases.

Another method is an exact line search, where the step size α varies between iterations. For the k-th iteration, the step size α is selected to minimize $-g(\lambda)$ along the direction $\lambda(k) - \alpha\, \partial g(k)$. That is,

$$\alpha(k) = \underset{\alpha}{\operatorname{argmin}} -g\big(\lambda(k) - \alpha\, \partial g(k)\big). \tag{4.25}$$

This method is often used when solving problem (4.25) costs less than computing $\partial g(\lambda)$. However, it is not very practical. Therefore, the backtracking line search is often used in practice. For each iteration, select a parameter $0 < \beta < 1$, then start with $\alpha = 1$ and update α with $\beta\alpha$ until

$$-g\big(\lambda(k) - \partial g(k)\big) \leq -g\big(\lambda(k)\big) - \frac{\alpha}{2}|\partial g(k)|^2. \tag{4.26}$$

It can be shown that the convergence rate with backtracking line search can be determined as

$$g(\lambda^*) - g\big(\lambda(k)\big) \leq \frac{|\lambda(0) - \lambda^*|^2}{2\alpha_{\min} k}, \tag{4.27}$$

where $\alpha_{\min} = \min\{1, \beta/L\}$.

For practical applications, many assumptions considered in the above will not be valid and the associated convergence analysis can become very challenging. It will be also very difficult to select an appropriate step size to guarantee convergence of the iterative algorithm.

4.3 Simulation Results

In this section, we provide simulation results to demonstrate the application of negotiation-based transactive energy systems to effectively coordinate and control distributed energy resources (DERs) and demand response (DR) for short-term scheduling and operation. More technical details and results can be found in (Wu et al. 2017). The control strategy proposed therein for integrated coordination between DERs and DR is shown in Figure 17, where a negotiation algorithm is adopted at the coordination layer, and a double-auction market is set up at the device layer for residential load aggregation. The simulation studies were performed on the Institute of Electrical and Electronics Engineers (IEEE) 123-node system and implemented in GridLAB-D.

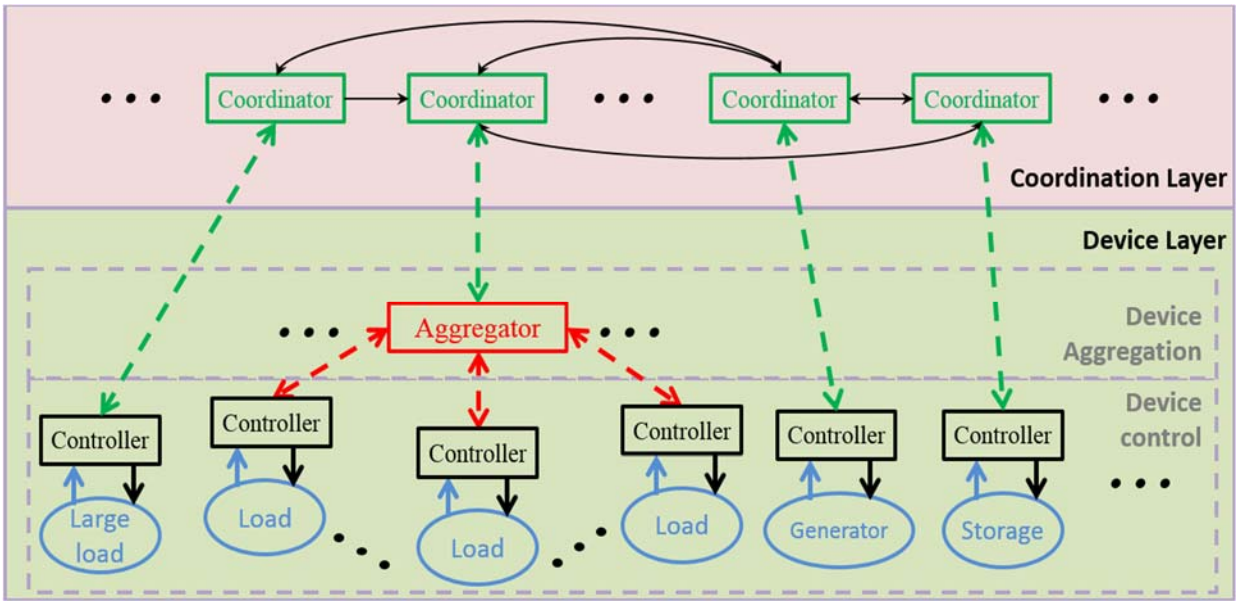

Figure 17. Hierarchical Control Framework for Integrated Coordination between DERs and DR

The IEEE 123-node test system shown in Figure 18 consists of 123 nodes and 118 lines. The nominal voltage of the feeder is 4.16 kV. It has been modified to include houses with air conditioners and other residential loads. The number of houses has been adjusted to match the peak load provided in the test system dataset, which results in 1,222 houses. There are 988 air conditioners participating in the DR program, and the remaining 234 air conditioners are uncontrollable, as are other residential loads. There are five distributed generators (DGs) connected to the system, whose cost parameters are listed in Table 1. The distributed algorithm for solving the optimal coordination problem is selected to be the leader-follower algorithm in (Kar and Hug 2012), which requires that (i) communication networks are undirected, and (ii) there is a leader that connects to all the remaining agents. The network assumes the star topology, where the center agent is associated with DG No. 1 and selected as the leader agent.

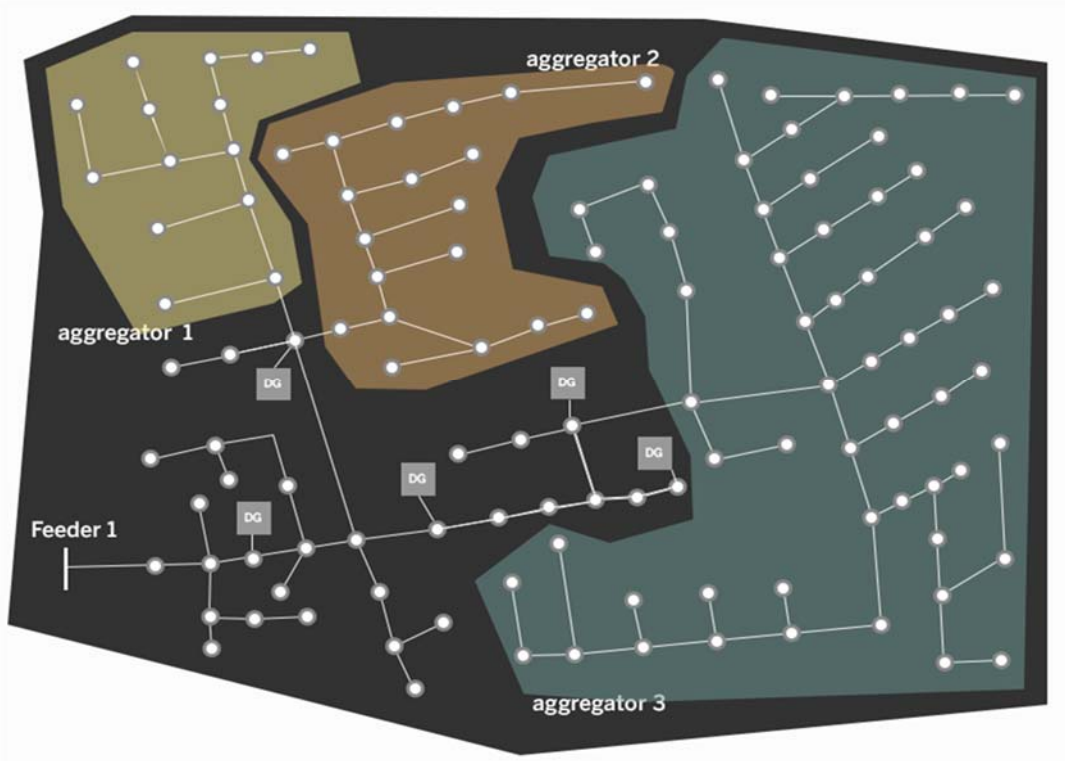

Figure 18. IEEE 123-Node Test System

Table 1. Generator Parameters

DG No.	a_i (\$/kW^{2}h)	b_i (\$/kWh)	c_i (\$/h)	Range (kW)
1	0.00015	0.0267	0.38	[50, 500]
2	0.00052	0.0152	0.65	[20, 100]
3	0.00042	0.0185	0.40	[40, 200]
4	0.00031	0.0297	0.30	[20, 250]
5	0.00025	0.0156	0.33	[30, 300]

The test system is first simulated without any DGs or controllable loads for a typical summer day. The 5-minute average feeder power consumption is plotted in Figure 19 together with the outside air temperature. Since air conditioners account for more than 80% of the total load in this system, the system load increases as the outside air temperature rises.

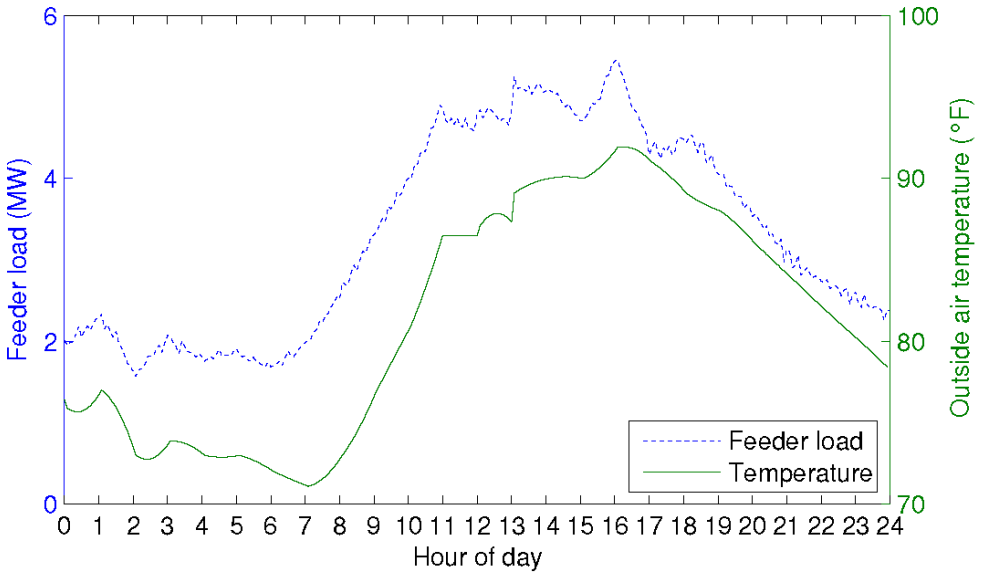

Figure 19. Base-Case Feeder Load (5-minute average) and Outside Air Temperature

The test system is then simulated with DGs and controllable loads under the proposed hierarchical control framework for the same summer day. In general, the reference signal can be any time series within the capability of the active distribution system. For the purpose of verifying the effectiveness of the proposed framework, the desired feeder load consumption is set to be 0.7 of the base-case feeder load, as shown by the blue dashed line in Figure 20. Such a reference signal is simple to construct yet useful to test the proposed method because

- The 30% reduction of load at the feeder requires the participation of DG and DR during scheduling.
- The reduction is proportional to the load feeder in the base case and therefore varies with time. Such varying load reduction requires DG and DR to vary their generation or consumption in a coordinated manner.
- Such a desired signal requires DG and DR to support the local system in peak hours more than in off-peak hours, which seems plausible. The test case enables us to compare DER participation in peak hours with off-peak hours, as well as the difference in energy price for the distribution system.

The obtained 5-minute average power consumption is plotted as the red curve in Figure 20. The actual feeder load follows the desired value within reasonable accuracy. The small mismatch is due to factors such as approximation of demand curve, errors in uncontrollable load forecast, and approximation of optimal solution in coordination layers.

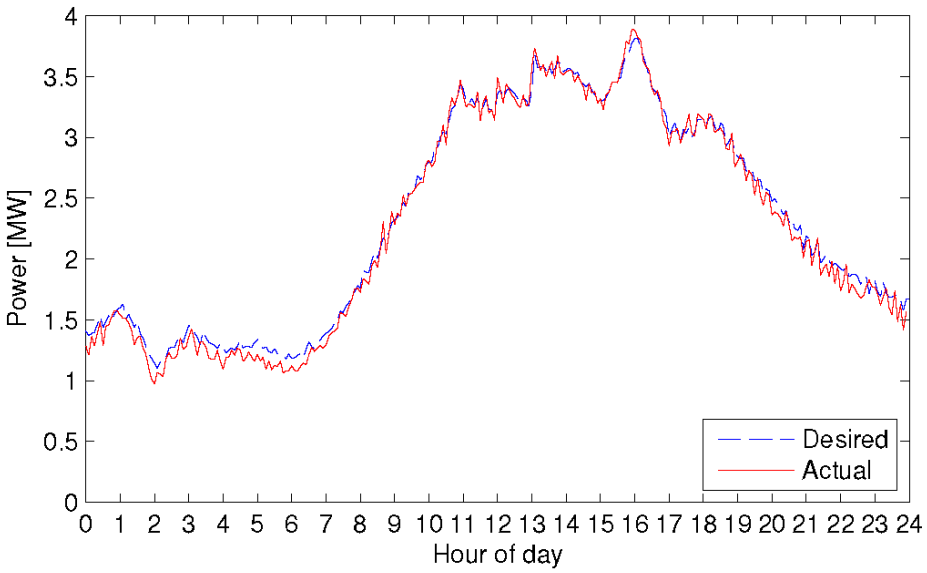

Figure 20. Desired vs. Resulting Feeder Load (both are 5-minute average)

The output of DGs is shown in Figure 21. DG2 is the cheapest generator and is at its maximum output almost all the time. Other DGs generate more in peak hours than in off-peak hours, because the reference signal essentially requires more reduction from the base case in peak hours. It can be easily verified that the marginal costs of all DGs that are not at their generation limits are the same, using the cost parameters in Table 1. The scheduled and actual loads from aggregators together with their dynamic capability (maximum and minimum) are plotted in Figure 22. The feasible load range for each air conditioner in each time period depends on the current indoor air temperature, temperature setpoint and acceptable range, price information, etc., and therefore varies much from one time period to another. Nevertheless, the feasible load range from the aggregation of a large number of air conditioners does not vary much. The actual average power consumption closely follows the desired value, which verifies the effectiveness of the proposed coordination and control.

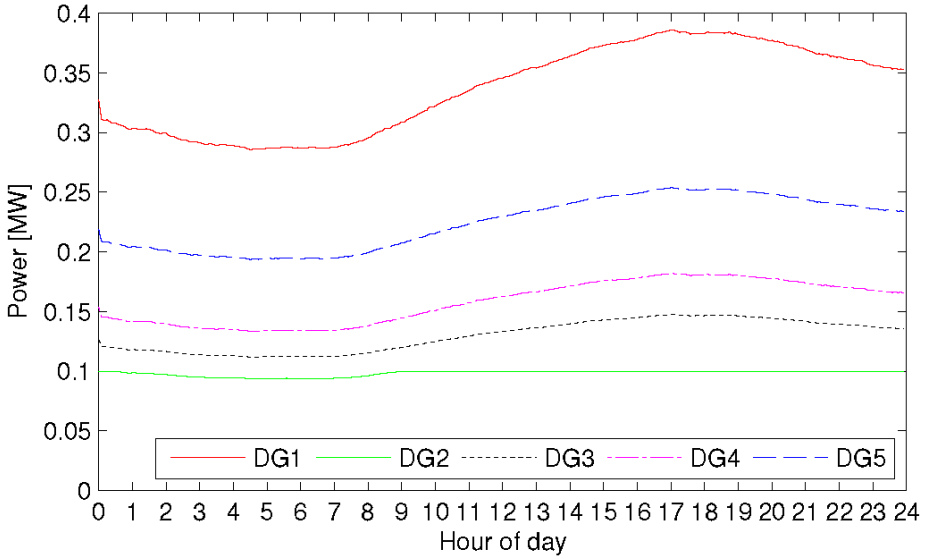

Figure 21. Generation Output from DGs

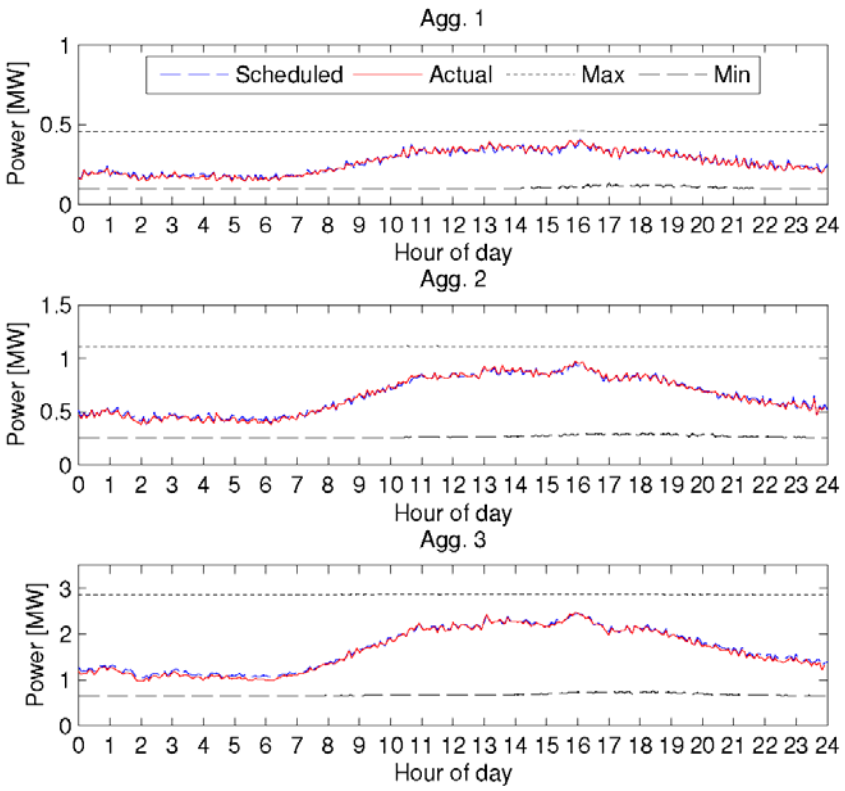

Figure 22. Load under Each Aggregator

The acceptable temperature settings and the simulated indoor air temperature are plotted in Figure 23 for a house under Aggregator 1. Based on how customers value their comfort, the temperature setpoint varies with the system energy cost throughout a day. During off-peak hours when the energy price is low, the temperature setpoint and indoor air temperature are closer to the desired one, which is 72.3°F in this case.

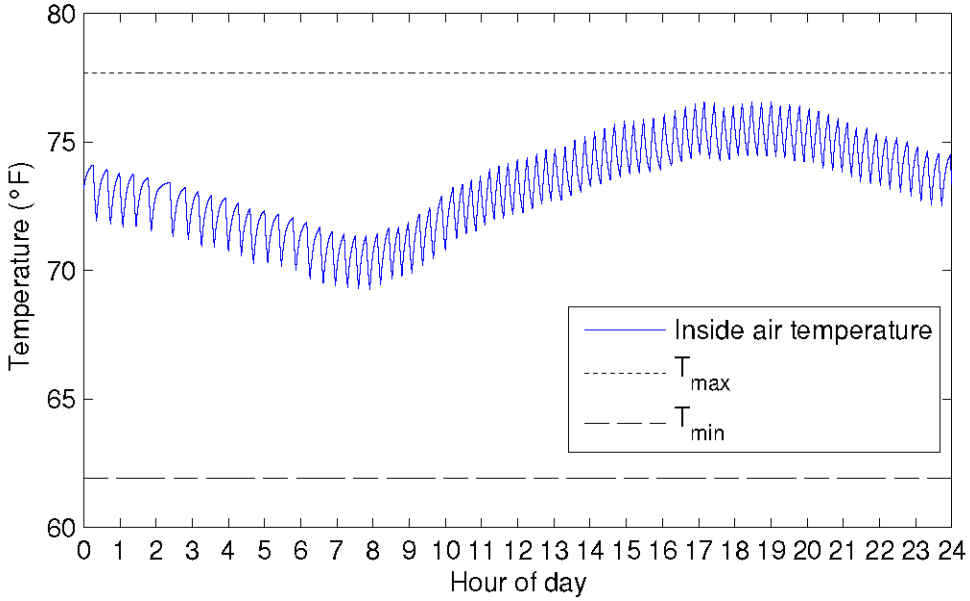

Figure 23. Indoor Air Temperature of a House under Aggregator 1

5.0 Conclusions and Future Work

In this report, we defined a set of quantitative and qualitative performance metrics in addition to the unified theoretical framework to characterize various transactive approaches from different perspectives. These performance metrics can be used to provide detailed insights into the effectiveness of various transactive designs and further identify their limitations. They can also provide guidance to improve the design of future transactive energy systems.

Then we applied the proposed theoretical framework to systematically analyze transactive energy systems deployed by the AEP gridSMART demonstration and a consensus method like that used in the Pacific Northwest Smart Grid Demonstration project. The proposed performance metrics were also used to investigate limitations of the transactive energy system using a double-auction market.

Our next step is to evaluate the performance and understand the limitations of the transactive energy system based on negotiation algorithms. Another future effort is to investigate price volatility and the potential load synchronization resulting from the design of a transactive energy system. In practice, load synchronization could be detrimental to frequency stability of the power grid.

6.0 References

Allcott, H. (2011). Rethinking real-time electricity pricing. *Resource and Energy Economics 33*(4), 820–842.

Bashash, S. and H. K. Fathy (2013, July). Modeling and control of aggregate air conditioning loads for robust renewable power management. *IEEE Transactions on Control System Technology 21*(4), 1318–1327.

Borenstein, S., M. Jaske, and A. Ros (2002, March). Dynamic pricing, advanced metering, and demand response in electricity markets. *Journal of the American Chemical Society 128*(12), 4136–4145.

Boyd, S. and L. Vandenberghe (2004). *Convex Optimization*. Cambridge, United Kingdom: Cambridge University Press.

Brooks, A., E. Lu, D. Reicher, C. Spirakis, and B. Weihl (2010, May–June). Demand dispatch. *IEEE Power Energy Magazine 8*(3), 20–29.

CAISO (2010, August). Integration of renewable resources: Operational requirements and generation fleet capability at 20% RPS. Technical report, California Independent System Operator.

Callaway, D. S. (2009, May). Tapping the energy storage potential in electric loads to deliver load following and regulation with application to wind energy. *Energy Conversion and Management 50*(5), 1389–1400.

Callaway, D. S. and I. A. Hiskens (2011, January). Achieving controllability of electric loads. *Proc. IEEE 99*(1), 184–199.

Chao, H. (2010). Price-responsive demand management for a smart grid world. *The Electricity Journal 23*(1), 7–20.

Chen, H., A. K. Coskun, and M. C. Caramanis (2013, December). Real-time power control of data centers for providing regulation service. In *Proc. 52nd IEEE Conference on Decision and Control*, pp. 4314–4321.

Chen, J., F. Lee, A. Breipohl, and R. Adapa (1995, November). Scheduling direct load control to minimize system operation cost. *IEEE Transactions on Power Systems 10*(4), 1994–2001.

Chen, L., N. Li, S. H. Low, and J. C. Doyle (2010, October). Two market models for demand response in power networks. In *Proc. 2010 First IEEE International Conference on Smart Grid Communications*, Gaithersburg, MD, pp. 397–402.

Chu, W. C., B. K. Chen, and C. K. Fu (1993, November). Scheduling of direct load control to minimize load reduction for a utility suffering from generation shortage. *IEEE Transactions on Power Systems 8*(4), 1525–1530.

Dominguez-Garcia, A. D., S. T. Cady, and C. N. Hadjicostis (2012). Decentralized optimal dispatch of distributed energy resources. In *Proc. 51st Annual Conference on Decision and Control*, pp. 3688–3693. IEEE.

EIA (2011, April). Annual Energy Outlook 2011 with Projection to 2035. Technical report, U.S. Energy Information Administration.

Fahrioglu, M. and F. L. Alvarado (2000, November). Designing incentive compatible contracts for effective demand management. *IEEE Transactions on Power Systems 15*(4), 1255–1260.

Faruqui, A., S. Sergici, and A. Sharif (2010). The impact of informational feedback on energy consumption: A survey of the experimental evidence. *Energy 35*(4), 1598–1608.

Fuller, J. C., K. P. Schneider, and D. Chassin (2011, July). Analysis of residential demand response and double-auction markets. In *Proc. 2011 IEEE Power and Energy Society General Meeting*, Detroit, MI, pp. 1–7.

Hammerstrom, D. J., R. Ambrosio, T. A. Carlon, J. G. DeSteese, G. R. Horst, R. Kajfasz, L. Kiesling, P. Michie, R. G. Pratt, M. Yao, J. Brous, D. P. Chassin, R. T. Guttromson, O. M. Jarvegren, S. Katipamula, N. T. Le, T. V. Oliver, and S. Thompson (2007, October). Pacific Northwest GridWise*TM* Testbed Demonstration Projects. Part I: Olympic Peninsula project. Technical Report PNNL-17167, Pacific Northwest National Laboratory.

Hammerstrom, D. J., D. Johnson, C. Kirkeby, Y. P. Agalgaonkar, S. T. Elbert, O. A. Kuchar, M. C. Marinovici, R. B. Melton, K. Subbarao, Z. T. Taylor, B. Scherer, S. Rowbotham, T. Kain, T. Rayome-Kelly, R. Schneider, R. F. Ambrosio, J. Hosking, S. Ghosh, M. Yao, R. Knori, J. Warren, J. Pusich-Lester, K. Whitener, L. Beckett, C. Mills, R. Bass, M. Osborne, and W. Lei (2015). Pacific Northwest Smart Grid Demonstration Project technology performance report Volume 1: Technology performance. Technical Report PNWD-4445, Battelle Memorial Institute.

Hogan, W. W. (2010). Demand response compensation, net benefits and cost allocation: Comments. *The Electricity Journal 23*(9), 19–24.

Huang, P., J. Kalagnanam, R. Natarajan, D. J. Hammerstrom, R. Melton, M. Sharma, and R. Ambrosio (2010, October). Analytics and transactive control design for the Pacific Northwest Smart Grid Demonstration project. In *Proc. 2010 First IEEE International Conference on Smart Grid Communications*, Gaithersburg, MD, pp. 449–454.

Kalsi, K., M. Elizondo, J. Fuller, S. Lu, and D. Chassin (2012, January). Development and validation of aggregated models for thermostatic controlled loads with demand response. In *Proc. 45th Hawaii International Conference on System Sciences*, Maui, HI.

Kar, S. and G. Hug (2012, July). Distributed robust economic dispatch in power systems: A consensus + innovations approach. In *Proc. 2012 IEEE Power and Energy Society General Meeting*, San Diego, CA, pp. 1–8.

Kok, K., B. Roossien, P. MacDougall, O. Pruissen, G. Venekamp, R. Kamphuis, J. Laarakkers, and C. Warmer (2012, July). Dynamic pricing by scalable energy management systems – Field experiences and simulation results using PowerMatcher. In *Proc. 2012 IEEE Power and Energy Society General Meeting*, San Diego, CA, pp. 1–8.

Kondoh, J., N. Lu, and D. J. Hammerstrom (2011, August). An evaluation of the water heater load potential for providing regulation service. *IEEE Transactions on Power Systems 26*(3), 1309–1316.

Kurucz, C., D. Brandt, and S. Sim (1996, November). A linear programming model for reducing system peak through customer load control programs. *IEEE Transactions on Power Systems 11*(4), 1817–1824.

Li, N., L. Chen, and S. H. Low (2011, July). Optimal demand response based on utility maximization in power networks. In *Proc. 2011 IEEE Power and Energy Society General Meeting*, Detroit, MI, pp. 1–8.

Li, S., M. Brocanelli, W. Zhang, and X. Wang (2014, September). Integrated power management of data centers and electric vehicles for energy and regulation market participation. *IEEE Transactions on Smart Grid 5*(5), 2283–2294.

Li, S., W. Zhang, J. Lian, and K. Kalsi (2016). Market-based coordination of thermostatically controlled loads Part I: A mechanism design formulation. *IEEE Transactions on Power Systems 31*(2), 1170–1178.

Liu, J., S. Li, W. Zhang, J. L. Mathieu, and G. Rizzoni (2013, December). Planning and control of electric vehicles using dynamic energy capacity models. In *Proc. 52nd IEEE Conference on Decision and Control*, pp. 379–384.

Makarov, Y., C. Loutan, J. Ma, and P. de Mello (2009, May). Operational impacts of wind generation on California power systems. *IEEE Transactions on Power Systems 24*(2), 1039–1050.

Mas-Colell, A., M. D. Whinston, and J. R. Green (1995). *Microeconomic theory*. New York, NY: Oxford University Press.

Mathieu, J. L., S. Koch, and D. S. Callaway (2013, February). State estimation and control of electric loads to manage real-time energy imbalance. *IEEE Transactions on Power Systems 28*(1), 430–440.

Samadi, P., H. Mohsenian-Rad, R. Schober, and V. W. S. Wong (2012, September). Advanced demand side management for the future smart grid using mechanism design. *IEEE Transactions on Smart Grid 3*(3), 1170–1180.

Smith, J., M. Milligan, E. DeMeo, and B. Parsons (2007, August). Utility wind integration and operating impact state of the art. *IEEE Transactions on Power Systems 22*(3), 900–908.

The GridWise Architecture Council (2015, January). GridWise transactive energy framework Version 1.0. Technical Report PNNL-22946, Pacific Northwest National Laboratory.

Vandael, S., B. Claessens, M. Hommelberg, T. Holvoet, and G. Deconinck (2013, June). A scalable three-step approach for demand side management of plug-in hybrid vehicles. *IEEE Transactions on Smart Grid 4*(2), 720–728.

Widergren, S. E., J. C. Fuller, M. C. Marinovici, and A. Somani (2014, February). Residential transactive control demonstration. In *Proc. 2014 Innovative Smart Grid Technologies Conference*, Washington, DC.

Widergren, S. E., K. Subbarao, J. C. Fuller, D. P. Chassin, A. Somani, C. Marinovici, and D. J. Hammerstrom (2014, February). AEP Ohio gridSMART Demonstration Project: Real-time pricing demonstration analysis. Technical Report PNNL-23192, Pacific Northwest National Laboratory.

Wu, D., J. Lian, Y. Sun, T. Yang, and J. Hansen (2017). Hierarchical control framework for integrated coordination between distributed energy resources and demand response. *Electric Power Systems Research 150*, 45 – 54.

Yang, T., J. Lu, D. Wu, J. Wu, G. Shi, Z. Meng, and K. H. Johansson (2016). A distributed algorithm for economic dispatch over time-varying directed networks with delays. *IEEE Transactions on Industrial Electronics*.

Zhang, W., J. Lian, C.-Y. Chang, and K. Kalsi (2013, November). Aggregated modeling and control of air conditioning loads for demand response. *IEEE Transactions on Power Systems 28*(4), 4655–4664.

Zhang, Z. and M.-Y. Chow (2011). Incremental cost consensus algorithm in a smart grid environment. In *Proc. 2011 IEEE Power and Energy Society General Meeting*, pp. 1–6. IEEE.

Zhang, Z. and M.-Y. Chow (2012a). Convergence analysis of the incremental cost consensus algorithm under different communication network topologies in a smart grid. *IEEE Transactions on Power Systems 27*(4), 1761–1768.

Zhang, Z. and M.-Y. Chow (2012b). The influence of time delays on decentralized economic dispatch by using incremental cost consensus algorithm. In *Control and Optimization Methods for Electric Smart Grids*, pp. 313–326. Springer.

Pacific Northwest
NATIONAL LABORATORY

Proudly Operated by **Battelle** *Since 1965*

U.S. DEPARTMENT OF
ENERGY

902 Battelle Boulevard
P.O. Box 999
Richland, WA 99352
1-888-375-PNNL (7665)

www.pnnl.gov